Transient Magnetic Field Effect of Photoexcitations in Donor–Acceptor Organic Semiconductors

Uyen N. V. Huynh[1, †], Tek P. Basel[1], Eitan Ehrenfreund[2], Zeev V. Vardeny[1]*

[1]*Physics and Astronomy Department, University of Utah, Salt Lake City, UT 84112, USA*

[2]*Physics Department, Technion Institute of Technology, Haifa 32000, Israel*

[†]*Current address: Cavendish Laboratory, Physics Department, University of Cambridge, Cambridge CB3 0HE, UK*

[*]*Correspondence to val@physics.utah.edu*

Abstract

We report transient photoinduced absorption (t-PA) and magnetic field (B) dependent t-PA (t-MPA(B)) in a pristine low bandgap π-conjugated copolymer composed of donor and acceptor moieties, namely poly[[4,8-bis[(2-ethylhexyl)oxy]benzo[1,2-b:4,5-b']dithiophene-2,6-diyl][3-fluoro-2-[(2-ethylhexyl)carbonyl]thieno[3,4-b]thiophenediyl]] (or PTB7) used in photovoltaic applications, which are measured in a broad time interval spanning eleven time decades, from 10^{-13} to 10^{-2} seconds and spectral range of 0.25-1.1 eV. Unlike traditional π-conjugated polymers in which the primary photoexcitations are singlet excitons (SE), in pristine PTB7 we find at short times coexistence of two primary photoexcitation species, namely SE and triplet-triplet (TT) pair. Both species are photogenerated directly from the ground state, and are spin-correlated. Although the TT pair decomposes into two separate triplet excitons (TE) in ~100 ps, nevertheless the separated TE spins are still entangled up to ~6 μs. At longer times, the t-MPA(B) response of the surviving TEs shows transient narrowing effect, which is attributed to a distribution of the TE size. In PTB7/PCBM blend used as active layer in organic solar cells we show that the SE dissociates into polaron pair (PP) at the copolymer/fullerene interface in less than ~5 ps, while the TT pair decomposition is faster compared to that in pristine PTB7. We also identify a back-reaction of the PP that acts as a loss mechanism in photovoltaic applications.

[†]Present address: Cavendish Laboratory, University of Cambridge CB3 0HE, UK.

I. Introduction

Recent advances in material synthesis have introduced a new class of organic semiconductors for organic photovoltaic (OPV) applications, namely the low bandgap π-conjugated copolymers with intrachain donor and acceptor moieties ("D-A copolymers") which already show power conversion efficiency (PCE) that exceeds 10% in a single layer bulk heterojunction organic photovoltaic (OPV) solar cell [1-3]. The advent of π-conjugated copolymers dates back to 2012 when a new D-A copolymer, namely the poly[[4,8-bis[(2-ethylhexyl)oxy]benzo[1,2-b:4,5-b']dithiophene-2,6-diyl][3-fluoro-2-[(2-ethylhexyl)carbonyl]thi-eno[3,4-b]thiophenediyl]]) that is known as PTB7, was introduced showing at the time a record PCE of 7.5% [1]. The field has evolved with a recent report of PCE approaching 11% in other D-A copolymers having similar backbone structure [2, 3]. We note in passing that the concept of internal D-A structure has also been applied to small molecules giving rise to the process of thermally activated delayed fluorescence that leads to record high internal quantum efficiency for organic light emitting diodes [4, 5], thus boosting their commercialization.

Recent spectroscopic and theoretical studies have indicated the possibility of intrachain 'singlet fission' in π-conjugated copolymers in the picosecond (ps) time domain[6-10] . However, the lack of optical probes in the mid-IR spectral range renders the identification of the primary photoexcitations in this class of materials difficult, especially because of their low bandgap[6, 8, 11] . Here we have conducted a comprehensive study of the primary and long-lived photoexcitations in thin films of pristine PTB7 using ultrafast transient photoinduced absorption (t-PA) focusing on the probe energy range in the mid-IR, namely 0.25-1.1 eV, in the broad time domain from sub-ps to millisecond, complemented by the time resolved magnetic field effect, dubbed t-MPA. We used these experimental methods to show that in PTB7 both singlet exciton (SE) and intrachain triplet-triplet (TT) pairs are simultaneously photogenerated leading to unique optical and magneto-optical responses. The TT pair decomposes into two separated triplet excitons (TE) in ~100 ps; however, the separated TE still maintain their spin entanglement up to ~6 μsec at low temperatures. The energy levels of the three types of photoexcited species, namely SE, TT and TE are shown schematically in Fig. 1d together with the possible TT decomposition scenario $TT \rightarrow (TE+TE)_{entangled} \rightarrow (TE+TE)_{separated}$. We also studied the photoexcitation dynamics in PTB7/fullerene blends used as active compound in OPV solar cells. We identify the SE

dissociation reaction at the copolymer/fullerene interfaces in less than 5 ps, which, in turn, accelerates the TT decomposition reaction. In addition, we also identify a back-reaction that is a loss mechanism for OPV cells. The main feature that enables the SE-TT coupling is the (near) energetic resonance between SE and TT; this feature is common to many other members of the class of π-conjugated D-A copolymers[12] in which the optical gap ranges between 1.5 eV to 1.8 eV.

II. Experimental

The PTB7 copolymer was bought from Sigma Aldrich. Pristine (or fullerene blend) films were prepared by drop cast or spin coating from a solution of pristine PTB7 (or PTB7/$PC_{71}BM$ blend) with mixing ratio 1:1.5 by weight dissolved in 1,2-dichlorobenzene (10mg/ml). Pristine 'isolated chain' PTB7 was prepared by mixing the PTB7 solution with polystyrene in 1,2-dichlorobenzene with the ratio of 1:1000 by weight. For the spectroscopic measurements the films were mounted inside a cryostat in vacuum of 10^{-4} torr. The external magnetic field of up to 300 mT was provided by an electromagnet, and the measurements were performed in the Voigt configuration, where the field was applied parallel to the film. Doping with iodine was accomplished by putting the pristine PTB7 film in a beaker having high iodine gas concentration, for about 2 minutes.

The t-PA picosecond set-up was described elsewhere[12, 13] ; it is a version of the well-known pump-probe correlation spectroscopy. The pump excitation beam was composed of pulses of 150 fs duration, 0.1 nJ/pulse, at 80 MHz repetition rate from a fs Ti:sapphire laser that was set at 1.6 eV photon energy. The initially photoexcited exciton density in the PTB7 copolymer film was adjusted to be ~$5x10^{16}$ cm^{-3}/pulse (assuming 100% photon to exciton conversion). The photoexcitation dynamics was measured by the changes, ΔT, caused by the pump excitation on the probe transmission, T. The probe spectral range, 0.55 eV to 1.05 eV, was generated by an OPO Ti:sapphire based laser (Spectra Physics) that delivers 'signal' and 'idler' beams. The probe spectral range was extended into the mid-IR from 0.25 eV to 0.43 eV by type I phase matching the "signal" and "idler" beams in a differential frequency crystal ($AgGaS_2$). The pump beam was modulated at frequency f=50 kHz, and the photoinduced absorption (PA≡ $-\Delta T/T$) was measured using an InSb detector (Judson IR) and a lock-in amplifier (SR830) set at f. A translation stage was introduced to the probe beam that could delay the probe pulses mechanically (1 ps=300 μm mechanical delay) thereby measuring the PA at time t set by the delay line. The t-PA spectrum

was then constructed from the t-PA measured at ~50 different wavelengths within the spectral range 0.25-1.05 eV.

For the t-PA spectroscopy in the μs time domain, the pulsed excitation was an OPO laser (Quanta-ray Indi model) that operates at 10 Hz repetition rate with 10 ns pulse duration. The 355nm OPA pump excited a basiScan OPO for generating pulses that are tunable across a broad spectral range from 410 nm to 2500 nm (0.5-3 eV). For the probe beam we have usually used an incandescent Tungsten/Halogen lamp followed by several band pass filters for monitoring the transient ΔT. The t-PA was monitored with a fast photodiode, namely InGaAs detector (Thorlabs), coupled to a data acquisition card ATS9462 with 100 MHz bandwidth. For this work the pump beam was set at 680 nm and $\Delta T(t)$ was measured at 980 nm using a laser diode, that was chosen to detect the TE species in the PTB7 copolymer. A potentiometer was set to 1 kΩ to establish the detector gain. The time response of this set up was < 0.5 μsec. For these measurements the pristine PTB7 films were mounted in a closed cycle He refrigerator cryostat, and the magnetic field was applied in the Voigt configuration. The transient measurements in the time interval of 0.5 to 400 μsec were limited to temperatures below 100 K, where the longer recombination times of the photoinduced species enabled reasonable magnitude for the t-MPA(B) (t-MPA> 0.1%). However all the measurements in the ps time domain (<2ns) were done at ambient conditions (namely at room temperature, RT), since the there is no S/N improvement for low temperature measurements in the ps time domain.

For the steady state PA measurements (ss-PA) a laser diode at 660 nm was used as a cw pump and an incandescent light (Tungsten Halogen) was used as a probe. The pump beam was modulated with a chopper at 300 Hz that was referenced to a lock-in amplifier. The probe beam was focused on the sample film, dispersed by a monochromator and detected by several semiconducting detectors such as Si, Ge and InSb. The PA was calculated as $-\Delta T/T$ after subtracting the photoluminescence emission from the sample. The measurements were performed at RT for the pristine copolymer films and at 40 K for the copolymer/fullerene blend.

III. Results and discussion

The chemical structure of PTB7 (see Fig. 1a inset) contains two different organic moieties, an electron rich (effectively acting as a "donor") and an electron "acceptor" in each unit cell[1, 14, 15] ,

which may slightly break the backbone inversion symmetry[6, 7, 9, 12] . The conjugation of D-A moieties leads to lower bandgap, extending to the near-IR range of the solar spectrum (<1.8 eV), and consequently improving the solar flux absorption, which is one ingredient that improve the OPV solar cell efficiency based on the PTB7 copolymer[1, 14, 16] . Figure 1a shows the absorption and photoluminescence spectra of pristine PTB7 film, that peak at 1.8 eV and 1.5 eV, respectively, with an apparent Stokes-shift of ~300 meV. The unusually large Stokes-shift, also found in other copolymers[12] , is bigger than that of traditional π-conjugated polymers such as DOO-PPV (a soluble derivative of the polymer poly-(p-phenylene-vinylene); PPV) and polythiophene derivatives, P3HT[17] .

To identify the lowest SE energy, E_{SE}, in the absorption spectrum we used the electro-absorption (EA) spectroscopy, since this type of modulation spectroscopy is more suitable to accurately determine transition energies. The PTB7 film in this case was deposited on interpenetrating gold electrodes, 50 μm apart, subjected to a 300 V voltage that was modulated at frequency f =500 Hz[18] ; whereas the EA was measured at 2f Figure 1(b) shows the EA spectrum of pristine PTB7 measured at 40 K. Two features dominate the EA spectrum. (i) The EA feature at low photon energy resembles the first derivative of the absorption spectrum at the band-edge, with a zero crossing energy at 1.8 eV, which is therefore assigned to the first excited state, S_1, of the copolymer. This is similar to the lowest SE, 1^1B_u, in traditional π-conjugated polymers, and thus the lowest SE energy in PTB7 is set at E_{SE}=1.8eV. (ii) The second dominant EA feature is an induced absorption band at 2.2 eV, which we assign to the m^1A_g state in the singlet manifold (see Fig. 1(d)). The m^1A_g is a dark, dipole forbidden, state in the absorption, which becomes accessible due to the electric field induced symmetry breaking. The energy difference, Δ_{SE} = E_{mAg}-E_{SE}= 0.4 eV is traditionally taken to be the lower bound of the exciton binding energy, E_b, in π-conjugated polymers; and we adopt this interpretation here for PTB7. We note that E_b of ~0.4 eV is much lower than E_b values in traditional polymers such as MEH-PPV and P3HT (~0.9eV)[13, 17, 19]. The lower E_b value here helps the exciton dissociation process, which facilitates charge photogeneration in this compound.

For identifying the long-lived photoexcitations in PTB7 such as TE and charge polarons, we have utilized the ss-PA[13, 20] . The ss-PA spectrum of the PTB7 film measured at 40 K is shown in Fig. 1c. The spectrum is dominated by a PA band, PA_T at 1.1 eV. We assign PA_T to optical

transitions in the triplet manifold of the PTB7 chain, namely the transition $1^3B_u \rightarrow m^3A_g$. This assignment is supported by the optically detected magnetic resonance response of the PA_T band, namely PADMR[21] , measured on the same film (see S.I. Fig. S1). Specifically, the PADMR(*B*) response of PA_T (where *B* is the magnetic field strength) exhibits typical triplet powder pattern which includes both full-field and half-field signatures[9, 12, 22] .

As determined from the PTB7 EA spectrum, the m^1A_g energy is $E(m^1A_g)\approx 2.2$ eV. Since in π-conjugated polymers the m^3A_g state is approximately 0.2 eV below that of the m^1A_g [20], we adopt this trend here and thus infer that $E(m^3A_g)\approx 2$ eV. Consequently, the TE lowest energy, E_{TE} can be determined from the relation $E_{TE}\equiv E(1^3B_u)=E(m^3A_g)-PA_T$. Using $PA_T=1.1$ eV from the ss-PA spectrum and $E(m^3A_g)\approx 2$ eV, we estimate $E_{TE} \approx 2\text{-}1.1= 0.9$ eV (see Fig. 1(d)). We therefore conclude that the lowest SE energy (E_{SE} =1.8 eV) is about twice that of the TE (E_{TE}=0.9 eV), paving the way for a resonant coupling between the SE and TT pair. Figure 1d shows the experimentally extracted energy diagram of SE, TE, and TT pair, in which the SE and TT energies are at resonance.

As shown previously[7, 12] , the TT state with an overall spin singlet but even orbital character could be directly photogenerated if the strict inversion symmetry in the copolymer is relaxed. Owing to the intrinsic D-A structure of the copolymer this condition may occur in PTB7 to some extend [7]. In the following we reveal the photogeneration process of the TT state.

The ps t-PA spectrum measured at RT in isolated chains of pristine PTB7 (0.1% of PTB7 embedded in polystyrene matrix by weight) is shown in Fig. 2a at various delay times, *t*. The spectrum is dominated by two PA bands peaking at PA_1=0.4 eV and PA_2=0.95 eV. This is in contrast to the t-PA spectrum of more traditional polymers such as DOO-PPV and P3HT, which show at t=0 only a single PA band that peaks at 0.95 eV (see Fig. S2). The low energy band, PA_1 was previously identified as due to the photogenerated SE absorption (PA_{SE}), since it is close to the energy difference $\Delta_{SE} = E_{mAg}\text{-}E_{SE}$ [20]. Recall also that from the EA spectrum (Fig. 1(b)) we estimated above $\Delta_{SE} = E_{mAg}\text{-}E_{SE}$=0.4 eV, thus we assign PA_1 to the absorption from the photogenerated SE in PTB7. However, the high energy band, PA_2, does not match any optical transition neither from the SE nor from TE (i.e. PA_T) which is ≈1.1 eV (Fig. 1c). In addition, at longer times, as PA_2 decays within 500 ps, it reveals a PA band very close to PA_T measured by ss-PA (Fig.2b). We therefore ascribe PA_2 in the t-PA spectrum of PTB7 to an optical transition

within the TT pair manifold, and mark it as PA_{TT}. Therefore, the blue-shift observed in the high energy PA delayed spectrum is due to spin conserving dissociation of the TT species into two separate TEs, namely ${}^1TT \rightarrow {}^1(TE + TE)$, where PA_{TT} of TT-pair transforms into PA_T of two separate TEs.

To better spectrally resolve the fast PA dynamics for energies around PA_2, the overlapping t-PA spectrum was decomposed into three PA bands, namely PA_{SE}, PA_{TT}, and PA_T for the photogenerated SE, TT pair and TE, respectively, using the generic algorithm (GA) method[23, 24] . Figure 2(b) shows the three decomposed PA bands and their associated dynamics (Fig. 2(b) inset). It is seen that the SE and TT species are instantaneously photogenerated within 300 fs time resolution, and their similar decay within ~200 ps generates the TE species. We therefore conclude that the TE in the ps time domain is in fact a by-product of the correlated TT and SE species. In the following, the t-MPA measurement in the ps time scale further strengthens this claim by revealing the spin correlation of these three species.

It might be argued that the 0.95 eV PA_2 band is the second optical transition of the SE species, provided that the rising and decay times of this band are the same as that of the 0.4 eV PA_{SE}. However, we show here that PA_2 in the picosecond timescale is highly susceptible to an applied magnetic field, **B,** suggesting that this band does not originate from a pure spin singlet state per-se. Rather, due to the resonant SE-TT coupling it is a nonzero spin species that may interact with the **B** field, resulting in a nonzero t-MPA response (see below for details). This strongly supports the assignment that PA_2 is due to instantaneous TT pair excitations, namely PA_{TT}.

Figure 2(c) shows the RT t-MPA(B) responses of both PA_{SE} and PA_{TT} bands, defined as t-MPA = [PA(t,B)- PA(t,0)]/PA(t,0), where PA(t,B) is the, SE or TT, PA(t) at field B, measured at t=200 ps. The ps resolved t-MPA(B) data shown in Fig. 2(c) is limited to B_{max}=0.3 T; it is thus sensitive to mechanisms for which the zero field splitting (ZFS) parameters of the system energy levels is $<\mu_B B_{max}$ [25] , but larger than ħ/t, where μB is the Bohr magneton. Such ZFS energies are typical [26] to TE and TT that are the main subject matter here. At larger fields, mechanisms caused by ZFS $<< \mu_B B_{max}$ saturate and mechanisms such as the Δg spin-mixing process take over[27, 28] . The t-MPA experiment was also attempted on the PA_{SE} band in DOO-PPV polymer. However, we found that there is no magnetic field effect within our 0.2% resolution at any t (see Fig. S2 inset). The null result shows that the SE in traditional π-conjugated polymers is not

susceptible to magnetic field, since it is not composed of non-singlet spin components. In contrast, the nonzero t-MPA for the PA_{SE} and PA_{TT} bands here show that both PA bands are susceptible to magnetic field. Importantly, PA_{TT} increases with *B*, whereas PA_{SE} decreases with *B* while having the same dynamics. The similar t-MPA time and field responses indicate that these two PA bands are correlated; namely *B* induces population increase of the TT excitation which comes *at the expense* of population decrease in the SE population. We therefore conclude that the t-MPA response of the PA_{SE} in PTB7 is a unique feature of the D-A copolymer with bandgap <2 eV[12] ; its correlated response with that of PA_{TT} is due to a resonance interaction between the SE and TT species.

This interaction was recently explained by a 'SE-TT model' using a spin Hamiltonian in 10-dimensional Hilbert space, where the Hamiltonian matrix is composed of 9x9 TT-pair matrix, 1x1 SE matrix, and coupling terms between various TT spin sub-states and the SE state[12] . The magnetic field changes the spin content of each of the 10 Zeeman separated levels. If the decay rates are spin dependent, then the spin densities of the SE and TT states change with time and field, which consequently induce the t-MPA(t,*B*) response. Figure 2d shows the t-MPA(t) evolution of the PA_{SE} and PA_{TT} bands at fixed field of *B*=300 mT; the two responses with opposite polarity increase with *B* up to 300 ps in the same manner. Importantly, there is no field-induced change of the initial population with *B*, namely t-MPA(t=0, B)=0, since the spin dependent recombination rates do not have the time to change the various SE and TT populations which induce t-MPA(B) response. As *t* increases, magnetic field dependent population variation due to spin dependent recombination rates gradually sets in, which leads to growing t-MPA response.

We also studied the photoexcitations dynamics in the microsecond to millisecond time domain using the μsec t-PA setup, which is based on transient electrical detection as described above. Figure 3(a) shows the t-PA dynamics at 980 nm up to 500 μsec at two fields: *B*=0 and *B*=180 mT measured at 40 K. We note that the *B*=0 dynamics cannot be fitted with a single exponential decay function. This indicates that the decay dynamics contains a distribution of recombination rates. A distribution in recombination rate is common to organic polymers having inhomogeneous structure.[29, 30] To show the influence of a distribution of recombination times on

the decay dynamics, we have succeeded in fitting the t-PA decay using a stretched exponential function,

$$PA(t) \propto N(t) = N_0 \exp(-(t/\tau_{eff})^{\beta}) \quad , \qquad (1)$$

with τ_{eff} = 6 ns and β=0.12 as shown in Fig. 3(a) inset. Such a function is typical to disordered systems with broad (~power law) recombination time distribution[31-34] .

As is clearly seen in Fig. 3(a) the applied magnetic field dramatically changes the t-PA dynamics; it increases the PA at early times but decreases it at later times starting from ~6 μsec. In order to trace the t-PA evolution with *B*, we measured the t-MPA(*B*) response at various delay times, as seen in Fig. 3(b). The t-MPA(*B*) response evolves from the non-saturated line shape that is similar to that of TT pairs in the ps time domain, to the line shape of individual, uncorrelated TE (Fig. 3(b)) that shows decrease at small *B* but saturates above a threshold *B* [35]. We attribute this line shape evolution to the loss of spin entanglement between the two geminate TEs born from the same TT photoexcitation species. As discussed above, the TT pairs are generated immediately following photon absorption. At longer time, of the order of ~100 ps, the TT pairs dissociate into 'spin-entangled' but separated intrachain TEs that keep their spin coherence up to ~6 μsec at low temperatures. At t>6 μsec the entanglement is gradually lost, even though the TEs recombine at much longer time, of the order of millisecond. At room temperature the spin lattice relaxation time is in general shorter (5-10 times shorter in polymers such as P3HT [36]), we therefore anticipate that the separated TEs would lose their spin entanglement at shorter times.

Surprisingly, the t-MPA(*B*) line-width of the non-entangled TEs (for t>6 μsec), as defined by the half width at half maximum (HWHM, Δ), also evolves with time (Fig. 3(b)). At t=20 μsec Δ ~20 mT; however with increasing *t*, Δ slowly decreases reaching ~6 mT at *t* =400 μsec (Fig. 3(c)). We found that Δ(t) dynamics are similar at 40K and 100K (Fig.3c); this indicates that motional narrowing mechanism is not the underlying mechanism for the Δ narrowing and we may find a different explanation. It is known [37] that Δ in MPA(B) responses is proportional to the TE's ZFS parameter, *D,* which in turn is determined by the e-h magnetic dipole-dipole interaction within the TE; namely $D=A/r^3$. In this way the narrowing in Δ(t) is related to having more TEs with larger size, *r* at longer times. This unexpected Δ dynamics can be explained by the TE size

distribution. From the distribution of the TE recombination times, discussed above, we infer that the TE size is also subjected to the inhomogeneity and disorder in the sample film. This correlation leads to a transient TE size, $r=r(t)$ for the surviving TEs, which may have longer recombination time that scales with r. As time progresses, the surviving TE population having longer recombination time also have larger size r, which, in turn shows narrower t-MPA response. This explains the observation of the narrowing t-MPA(B) response with time, validating our TE size distribution approach. From the measured $\Delta(t)$ dynamics presented in Fig. 3(c) we estimate that Δ decreases by only a factor of three as the delay time changes by a factor of 20 (namely from 20 to 400 μs), implying a very slow $r(t)$ increase. We therefore try a logarithmic behavior; we assume that for $t>t_0$ the TE size $r(t)$ depends logarithmically on time,

$$r(t) = r_0(1 + \alpha \ln(t / t_0)), \qquad (2)$$

where $t_0<20$ μsec, and $r_0=r(t=t_0)$ and α are sample specific parameters. Equation (2) is expected to be valid for $t<t_{max}$, beyond which r remains constant. Figure 3(c) shows that the measured $\Delta(t)$ can be simulated using Eq. (2) and assuming that $\Delta \propto D \propto r^{-3}$; this fit supports our conjecture that the TE size of the surviving TEs grows slowly with time.

It is interesting to understand the role played by the TT photoexcitation species in the charge photogeneration process in PTB7/$PC_{71}BM$ blend, where the copolymer acts as a donor and the fullerene molecule is an acceptor. For studying the charge photogeneration process we first identify the absorption characteristics of the charge photoexcitations in the copolymer by measuring the absorption spectrum of the pristine PTB7 film doped with iodine vapor. The absorption spectrum of the iodine doped film, namely doping induced absorption or DIA, measured at RT using a CARY 17 spectrophotometer, is shown in Fig. 4(a). It consists of two dominant DIA bands at 0.3 eV and 1.1 eV, respectively, which are equivalent to the two optical transitions P_1 and P_2 of charge polarons[12] ; these bands are accompanied by DIA of IR-active vibrations with large oscillator strength. Figure 4(b) shows the ss-PA spectrum of a PTB7/$PC_{71}BM$ blend film measured at 40 K. The PA spectrum shows two bands at 0.35 eV and 1.1 eV that are characteristic of the polaron bands P_1 and P_2 seen in the DIA spectrum. However, since the PA_T band is also peaked at 1.1eV (Fig. 1(c)), the 1.1 eV PA band here may have two

separate contributions from two different photoexcitation species, namely PA_T from TEs and P_2 from charge polarons; whereas the 0.35 eV PA band is assigned only to the lower P_1 transition. This explains the different relative strength of the 1.1 and 0.35 eV bands in the DIA and ss-PA spectra, when comparing Figs. 4(a) and 4(b), respectively.

Next, we probe the photoexcitation dynamics in the PTB7/PCBM blend using the t-PA technique. Figure 4(c) illustrates the t-PA spectrum at various time delays in the copolymer/fullerene blend in the ps time domain measured at RT. At t=0 the t-PA spectrum is similar to that in the pristine PTB7 film that consists of the two PA bands PA_{SE} at 0.4 eV and PA_{TT} at 0.95eV. At t>0 the t-PA spectrum evolves, showing a blue-shift of the PA_{TT} towards $PA_T + P_2$ bands, and red-shift of the PA_{SE} towards P_1. As seen in Fig. 4(d), the TT band decays quickly within 20 ps into a plateau, whereas at the same time the $PA_T + P_2$ bands increase. We therefore attribute the blue-shift of the TT band to the decomposition of the TT pair into separate TEs, which occurs much faster in the blend compared to the pristine PTB7 film. Meanwhile, the decay of PA_{SE} that leads to the formation of the P_1 band shows the dissociation of the SE into PP ($SE \rightarrow {}^1PP$) across the interface of the PTB7/PCBM.

The t-PA dynamics however continues to evolve after the TT→2TEs decomposition. In fact, PA_T *increases* from *t*=20 ps up to *t*=1 ns, as seen in Fig 4(d). We interpret this increase due to PP 'back-reaction' into TE on the copolymer chains[23]. Since the TE in the copolymer is quite stable in the blend film, this back-reaction channel is one of the main loss mechanisms for charge extraction in OPV devices based on the π-conjugated copolymers, which may limit the PCE of the solar cell devices. Alas, we anticipate that this back reaction loss would be more effective in copolymers with smaller energy gap, since the lowest TE state in such copolymers would increase, and thus the PP→TE reaction may be more effective.

Our spectroscopic study of PTB7 copolymer and its blend with PCBM fullerene may help designing other copolymers which may improve the PCE of OPV solar cells, since we identified loss channels for charge photogeneration and extraction. First, the long lived (up to hundreds of microseconds) TEs in the copolymer chains need be considered as a loss for efficient solar cells. Second, the early photogeneration of the TT state might not be beneficial to the photocurrent as the TT dissociation into TEs is accelerated in the blend, and this is another loss channel. We note, however that the main loss channel due to PPs back recombination into TEs in the

copolymers may be controlled by adding a small fraction of spin ½ radical additives as reported in ref. [22].

IV. Conclusions

In summary, we used the t-PA and t-MPA responses in a broad spectral range and time domain for studying the photoexcitations dynamics in pristine PTB7, a low band-gap π-conjugated copolymer, as well as in PTB7/PCBM blend. We identified a second mid-IR PA band in the ps time domain that originates from TT-pair species, which is unique to π-conjugated copolymers. It is instantaneously photogenerated, simultaneously with that of the singlet exciton, but its decay dynamics are correlated with the generation of triplet excitons. This indicates that the decomposition reaction, namely intrachain singlet fission, TT→ TE↑ + TE↓ occurs within ~100 ps. Moreover, due to the resonance between the SE and TT-pair energies, there is a spin-correlation between the two species which leads to t-MPA in the ps time domain. When using the t-MPA technique in the μsec time scale, we showed that the decomposed geminate TEs are still spin-entangled up to ~6 μsec at low temperatures < 100 K. We anticipate shorter spin coherence duration at room temperature due to shorter spin lattice relaxation times. In addition, we measured a transient narrowing effect for the surviving TEs t-MPA(*B*) response, that we can explain by a distribution of TE decay times in the disordered film, which leads to slight expansion of the surviving TEs size with time. In the PTB7/PCBM blend we identified the SE→ ^{1}PP dissociation reaction at the copolymer/fullerene interfaces. This reaction may accelerate the parallel TT decomposition rate into separate TEs. In addition, some fraction of the photogenerated PP species density undergoes a back-reaction process of ^{3}PP→TE, which is considered to be a loss mechanism to OPV solar cells. Our results should not be unique to PTB7 copolymer; in fact similar photoexcitations dynamics may occur for other π-conjugated copolymers having energy gap < 2 eV.

Acknowledgements

This work was supported by the AFOSR under award number FA9550-16-1-0207 (ps transient spectroscopies) and NSF DMR-1701427 (cw spectroscopies). The work at Technion was supported by the Israel Science Foundation (ISF 598/14).

References:

1. Y. Liang, Z. Xu, J. Xia, S.-T. Tsai, Y. Wu, G. Li, C. Ray and L. Yu, Adv Mater **22**, E135-E138 (2010).
2. Y. Liu, J. Zhao, Z. Li, C. Mu, W. Ma, H. Hu, K. Jiang, H. Lin, H. Ade and H. Yan, Nature Communications **5**, 5293 (2015).
3. Z. He, B. Xiao, F. Liu, H. Wu, Y. Yang, S. Xiao, C. Wang, T. P. Russell and Y. Cao, Nature Photonics **9** (3), 174-179 (2015).
4. H. Uoyama, K. Goushi, K. Shizu, H. Nomura and C. Adachi, Nature **492** (7428), 234-238 (2012).
5. K. Goushi, K. Yoshida, K. Sato and C. Adachi, Nature Photonics **6** (4), 253-258 (2012).
6. Y. Kasai, Y. Tamai, H. Ohkita, H. Benten and S. Ito, J. Am. Chem. Soc. **137**, 15980 (2015).
7. K. Aryanpour, T. Dutta, U. V. Huynh, Z. V. Vardeny and S. Mazumdar, Phys. Rev. Letters **115**, 267401 (2015).
8. E. Busby, J. Xia, Q. Wu, J. Z. Low, R. Song, J. R. Miller, X-Y. Zhu, L. M. Campos and M. Y. Sfeir, Nat Mater **14**, 426-433 (2015).
9. U. Huynh, T. Basel, T. Xu, L. Lu, T. Zheng, L. Yu and Z. V. Vardeny, SPIE NanoScience and Engineering (International Society for Optics nd Photonics), 91650Z (2014).
10. D. Di, A. S. Romanov, L. Yang, J. M. Richter, J. P. Rivett, S. Jones, T. H. Thomas, J. M. Abdi, R. H. Friend, M. Linnolahti, M. Bochmann and D. Credgington, Science **356**, 159-163 (2017).
11. M. S. Menke and e. al, ACS nano **10**, 10736-10744 (2016).
12. U. N. V. Huynh, T. P. Basel, E. Ehrenfreund, G. Li, Y. Yang, S. Mazumdar and Z. V. Vardeny, Phys. Rev. Letters **119**, 017401 (2017).
13. T. Drori, J. Holt and Z. V. Vardeny, Phys. Rev. **B82**, 075210 (2010).
14. R. Tautz, E. D. Como, T. Limmer, J. Feldmann, H.-J. Egelhaaf, E. V. Hauff, V. Lemaur, D. Beljonne, S. Yilmaz and I. Dumsch, Nat Commun **3**, 970 (2012).
15. L. Dou, C.-C. Chen, K. Yoshimura, K. Ohya, W.-H. Chang, J. Gao, Y. Lin, E. Richards and Y. Yang, Macromolecules **46**, 3384 (2013).
16. R. S. Kularante, H. D. Magurudeniya, P. Sista, M. C. Biewer and M. C. Stefan, J. Polym. Sci. Part A: Polym. Chem. **51**, 743 (2013).
17. Z. V. Vardeny and M. Wholgenannt, in *Semiconducting Polymers*, edited by G. Hadziioannou and G. G. Malliaras (WILEY-VCH, 2007), pp. 235-275.
18. M. Liess, S. Jeglinski, Z. V. Vardeny, M. Ozaki, K. Yoshino, Y. Ding and T. Barton, Phys. Rev. **B56**, 15712 (1997).
19. M. Chandross and S. Mazumdar, Phys. Rev. **B55**, 1497 (1997).
20. S. Frolov, Z. Bao, M. Wholgenannt and Z. V. Vardeny, Phys. Rev. Letters **2000**, 2196 (2000).
21. P. A. Lane, J. Shinar and K. Yoshino, Phys. Rev. **B54**, 9308 (1996).
22. T. Basel, U. Huynh, T. Zheng, T. Xu, L. Yu and Z. V. Vardeny, Adv. Func. Mater. **25**, 1895 (2015).
23. A. Rao, P. C. Y. Chow, S. Gelinas, C. W. Schlenker, C.-Z. Li, H.-L. Yip, A. K.-Y. Jen , D. S. Ginger and R. H. Friend, Nature **500**, 435-440 (2013).

24. S. Gélinas, O. Paré-Labrosse, C.-N. Brosseau, S. Albert-Seifried, C. R. McNeill, K. R. Kirov, I. A. Howard, R. Leonelli, R. H. Friend and C. Silva, J. Phys. Chem. C **115**, 7114-7119 (2011).
25. H. Hayashi, *Introduction to dynamic spin chemistry; magnetic field effects on chemical and biochemical reactions*. (World Scientific Publishing Co., Singapore, 2004).
26. X. Wei, B. C. Hess, Z. V. Vardeny and F. Wudl, Phys Rev Lett **68**, 666-669 (1992).
27. A. H. Devir-Wolfman, B. Khachatryan, B. R. Gautam, L. Tzabary, A. Keren, N. Tessler, Z. V. Vardeny and E. Ehrenfreund, Nat Commun **5**, 4529 (2014).
28. B. Khachatryan, A. H. Devir-Wolfman, L. Tzabari, N. Tessler, Z. V. Vardeny and E. Ehrenfreund, Phys. Rev. Applied **5** (4), 044001 (2016).
29. O. Epshtein, G. Nakhmanovich, Y. Eichen and E. Ehrenfreund, Phys. Rev. B **63**, 125206 (2001).
30. O. Epshtein, Y. Eichen, E. Ehrenfreund, M. Wohlgenannt and Z. V. Vardeny, Phys. Rev. Letters **90**, 046804 (2003).
31. G. Zatryb, A. Podhorodecki, J. Misiewicz, J. Cardin and F. Gourbilleau, Nanoscale Res. Lett. **6**, 1 (2011).
32. G. Pfister and H. Scher, Advances in Physics **27**, 747-798 (1978).
33. F. Alvarez, A. Algeria and J. Colmenero, Phys. Rev. B **44**, 7306-7312 (1991).
34. J. C. Phillips, Chem. Phys. **212**, 41 (1996).
35. B. R. Gautam, T. D. Nguyen, E. Ehrenfreund and Z. V. Vardeny, Phys. Rev. B **85**, 205207 (2012).
36. V. I. Krinichnyi, P. A. Troshin and N. N. Denisov, Acta Materialia **56**, 3982–3989 (2008).
37. R. E. Merrifield, Pure and Applied Chemistry **27**, 481-498 (1971).

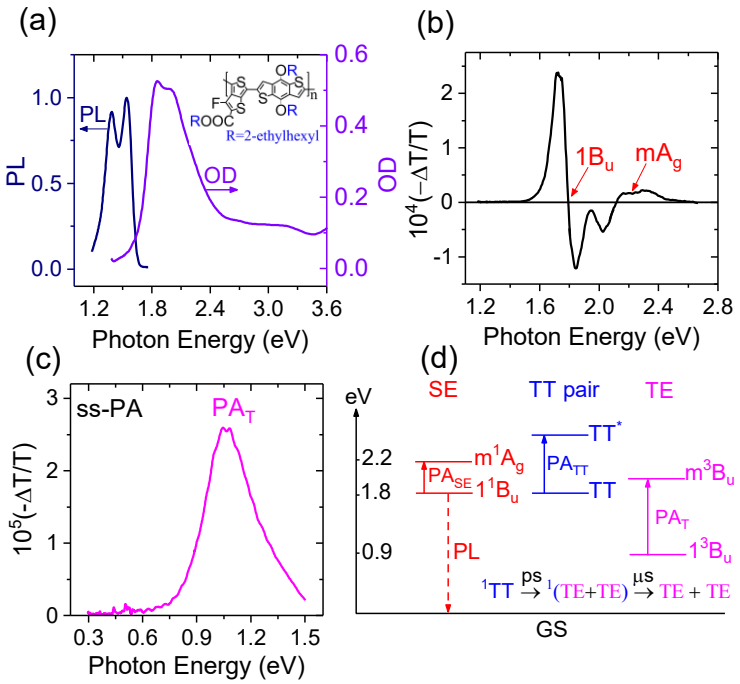

Figure 1| (color online): Steady state optical spectroscopies of pristine PTB7. (a) The absorption and photoluminescence spectra of the PTB7 film at RT; the inset shows the copolymer chemical structure. (b) The electroabsorption (EA) spectrum of PTB7 film measured at 40 K; the EA features $1B_u$ and mA_g are denoted. (c) Steady state photoinduced absorption (ss-PA) of PTB7 measured at RT, where the TE band, PA_T is assigned. (d) Energy diagram of SE, TT, and TE manifolds, where various optical transition bands are denoted. The dissociation reaction of TT into two geminate spin entangled TEs in the picosecond time domain, and the gradual loss of spin coherence of the geminate TEs in microsecond time is also indicated.

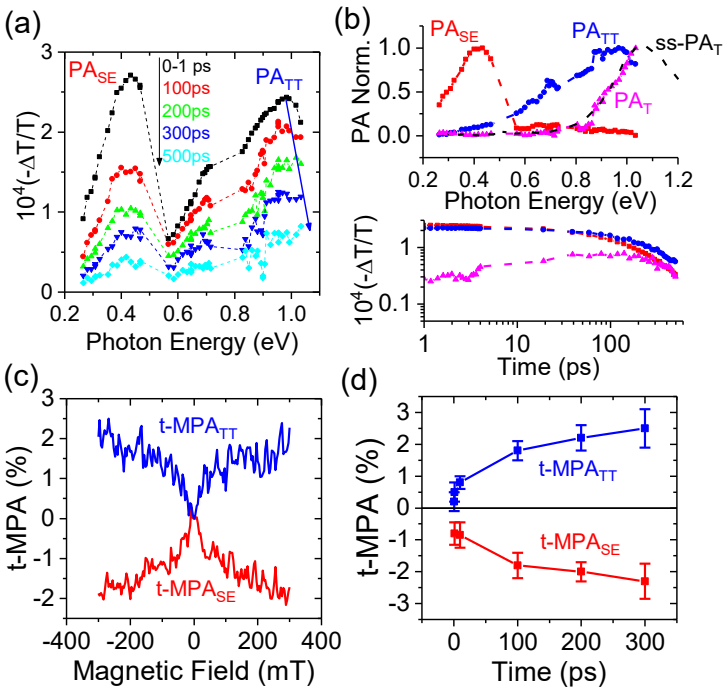

Figure 2| (color online): Room temperature transient picosecond photoinduced absorption (t-PA) and magneto photoinduced absorption (t-MPA) spectroscopies of PTB7 isolated chains in polystyrene, excited at 775 nm. (a) The ps t-PA spectrum evolution of the isolated chain PTB7 where two PA bands are assigned. (b) Upper panel: three decomposed spectra PA_{SE} (red rectangles), PA_{TT} (blue dot), and PA_T (magenta triangle) using the GA method (see text). The steady state PA_T band (black dashed curve) is also shown for comparison. Lower panel: time evolution of the SE, TT, and TE bands, respectively. (c) t-MPA(B) responses of PA_{TT} and PA_{SE} bands measured at t = 200 ps delay time. (d) t-MPA responses of PA_{TT} and PA_{SE} measured at a fixed field B = 300 mT.

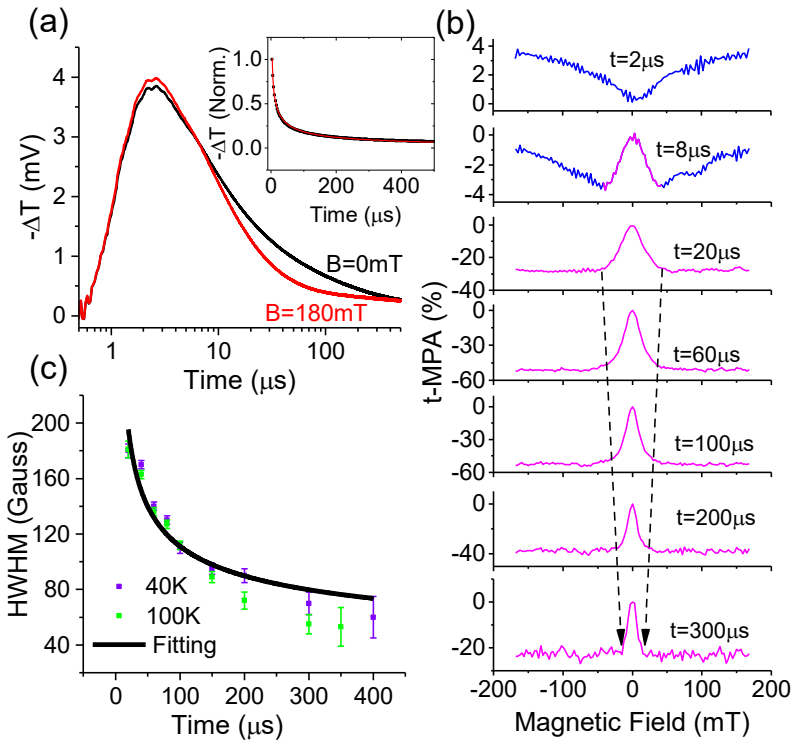

Figure 3| (color online): t-PA and t-MPA dynamics of PTB7 pristine films excited with 10 ns pulse at 660 nm and probed at 980 nm measured at 40 K. (a) μs dynamics at B=0 (black) and B=180 mT (red). The zero field dynamics seen in the inset is fitted using a stretched exponential decay function (inset, red line through the data). (b) μs t-MPA(B) responses at different delay times measured at 40 K. (c) The HWHM of the t-MPA response as a function of delay time measured at 40 K and 100 K, and a fit (black curve) based on a model discussed in the text.

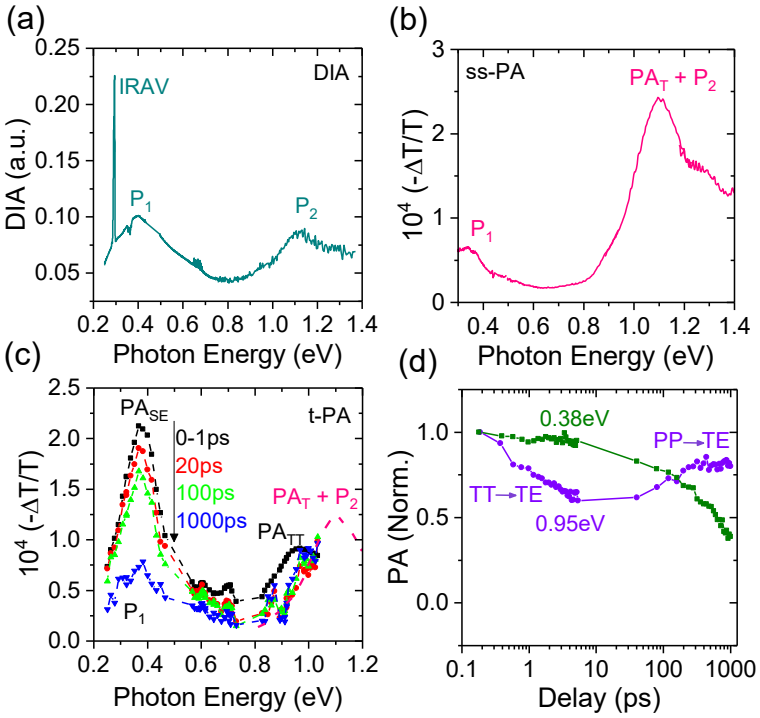

Figure 4| (color online): Photoexcitations dynamics in PTB7/$PC_{71}BM$ blend. (a) Doping induced absorption spectrum of PTB7 doped with iodine vapor for two minutes measured at RT. Two electronic bands, P_1 and P_2, and vibrational bands (IR-active vibrations; IRAV) are assigned. (b) Steady state PA of PTB7/$PC_{71}BM$ blend film measured at 40 K. Two PA bands due to polarons, P_1, P_2, and PA_T of TE are assigned. (c) Picosecond transient PA spectral evolution at various delay times', measured at RT. Various PA bands are assigned. (d) RT decay kinetics measured at 0.38 eV and 0.95 eV probes that show two different processes as denoted. (i) TT decomposition into TEs for t<5 ps; and (ii) back-reaction of PP→TE for t>50 ps.